Controlled Formation of Mass-Selected Cu−Au Core−Shell Cluster Beams

Feng Yin, Zhi Wei Wang, and Richard E. Palmer*

Nanoscale Physics Research Laboratory, School of Physics and Astronomy, University of Birmingham, Birmingham B15 2TT, U.K.

ABSTRACT: Synthesis of bimetallic clusters is a topic of accelerated interest; their physical and chemical properties are greatly dependent on their composition, size, and structure. The cluster beam technique is widely used for preparation of clusters. However, creating bimetallic clusters with well-controlled composition, size, and structure, especially for larger clusters (>100 atoms), is still a big challenge. Here we demonstrate that not only size and composition but also the structure of bimetallic clusters can be controlled by tuning aggregation parameters.

Figure 1. STEM images and diameter distributions of two mass-selected bimetallic Au−Cu clusters samples: (a,c) sample deposited under 500 sccm/205 sccm He/Ar flow and 1.0 mbar aggregation pressure; (b,d) sample deposited under 88 sccm/178 sccm He/Ar flow and 0.34 mbar aggregation pressure.

Bimetallic nanoparticles display new properties, which cannot be obtained by varying either the size of the pure metallic systems or the composition of bulk bimetallic alloys.[1−5] Bimetallic core/shell clusters offer fascinating prospects for the design of selective catalysts[1−4,6−10] as well as optical[2−5,11,12] and magnetic[3,4,13−15] systems. Such bimetallic clusters can be created by a variety of techniques including chemical reduction and electrochemical synthesis etc.[1−17] The advantage of the cluster beam technique is that it enables the generation of model catalysts with precise, atomic-scale size control.[18−28] However, cluster beam synthesis of nanoparticles of well-controlled size, composition, and structure is extremely challenging for clusters containing more than ∼100 atoms, primarily because of limitation in the transmission of the mass-spectrometers used to select the particle size. Here, we demonstrate the controlled cluster beam synthesis of both Cu rich/Au rich and Au rich/Cu rich mass-selected core/shell clusters containing several thousand atoms. The experiment employs an Au−Cu alloy target and our unique lateral time-of-flight mass spectrometer.[20,22,29−31] The clusters were analyzed by aberration-corrected scanning transmission electron microscopy (STEM).[32,33] The results provide insight into the growth kinetics of the bimetallic clusters leading to the controlled, selective and efficient production of a different metastable but practical core/shell nanoparticle morphologies.

We focus on mass-selected Au−Cu bimetallic clusters (mass = 222 250 Da) created in a home-built RF magnetron sputtering gas condensation cluster beam source with lateral time-of-flight mass filter[28−31] from an Au−Cu mixed target (molar ratio, Au: Cu = 10:90). The clusters were deposited at low energy (500 eV) on TEM grids covered with amorphous carbon film. (sample A was deposited under 500 sccm/205 sccm He/Ar flow and 1.0 mbar aggregation pressure; sample B was deposited under 88 sccm/178 sccm He/Ar flow and 0.34 mbar aggregation pressure.) The STEM characterization was performed with a 200 kV JEM 2100F instrument equipped with a probe corrector (CEOS GmbH) and high-angle annular dark-field (HAADF)
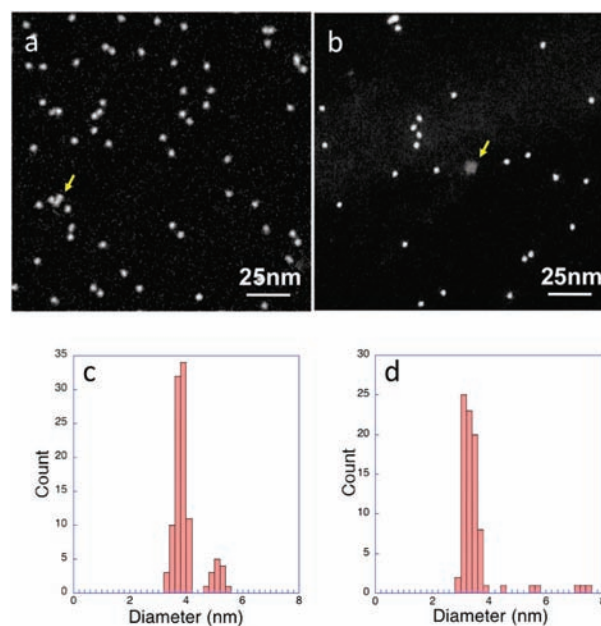
detector, with inner and outer collection angles of 62 and 164 mrad in these experiments.

Figure 1 shows representative STEM images and diameter distributions of two illustrative, mass-selected bimetallic cluster samples. The principal difference between the synthesis conditions was the flow rate of the condensation gas (He) and thus also the aggregation pressure in the cluster source. (For details please see caption to Figure 1.) Most clusters in the high He flow/pressure sample, Figure 1a, have uniform contrast and size; a few clusters which have coalesced, as marked by the arrow. The corresponding diameter distribution, Figure 1c, has a bimodal distrbution. The first peak is strong and narrow with an average diameter of 3.78 ± 0.19 nm (standard deviation is used for estimating of the error bars), the second is weak and is centered around 5.2 nm, probably arising from some cluster aggregation after deposition. As shown in Figure 1b, the low pressure exhibits two kinds of clusters. The large majorities are bright in contrast and uniform in size; the remaining few are dark and large (marked by arrow). The lower HAADF intensity, suggests these rare, large clusters are pure Cu
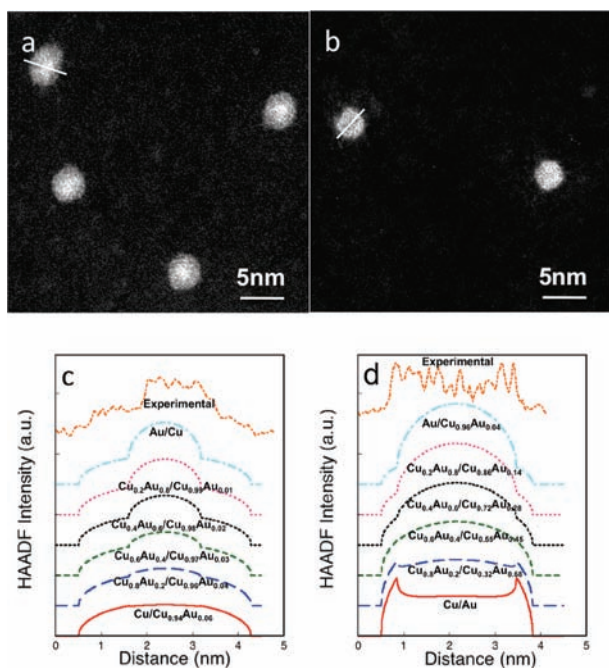
Figure 2. High-resolution STEM images, simulated and experimental HAADF intensity line profiles for two mass-selected bimetallic Au−Cu clusters samples: (a,c) sample deposited under 500 sccm/205 sccm He/Ar flow and 1.0 mbar aggregation pressure; (b,d) sample deposited under 88 sccm/178 sccm He/Ar flow and 0.34 mbar aggregation pressure.

(or Cu rich), reflecting the Z-contrast mechanism.[4,5,32−35] The diameter of the majority of clusters formed at low He flow/pressure sample, Figure 1d, is smaller than that of the high He flow/pressure sample. The average diameter is 3.32 ± 0.21 nm. Because the mass of Au and Cu atoms is 197 and 63.5 Da, respectively, in order to keep the mass of particles constant, one extra/less Au atom in the cluster should induce three Cu atoms less/more. Moreover, the difference in radius between Au (1.44 Å) and Cu (1.28 Å) atoms is <12.5%.[36] The composition change of the cluster should lead to the size change. The narrow distribution suggests that these clusters have similar composition as well as mass selected. Because we know the mass of the particles, the atomic composition of the two samples can be quantified with a simple hardball model. This gives Au composition ratio of about 5% for the high He flow/pressure sample, which is a slightly lower than the composition of the target (10%). However, at low pressure the Au ratio increases to about 43%, much higher than the composition of the target. This result shows that the atomic composition of the clusters can be tuned by control of the aggregation parameters in conjunction with the mass-selection.

Figure 2 displays high-resolution aberration corrected STEM images of the two samples. The HAADF image contrast is proportional to Z^n, where Z is the atomic number and we have assumed that n is 1.32,[33] so chemical contrast can be obtained. We can see that the structures of the clusters synthesized at different pressure are quite different. In the high He flow/pressure sample, Figure 2a, the central parts of the clusters are obviously brighter. In the low He flow/pressure sample, Figure 2b, the central areas of clusters are either similar to or darker than the edge areas. The difference in intensity contrast between the two types of cluster can be seen especially clearly in

the corresponding line profiles, Figure 2c ,d. In Figure 2c we can see that the intensity increases abruptly 2.3 times as we approach the center, whereas in Figure 2d, a reduced intensity is apparent at the center. The atomic numbers of Cu and Au are 29 and 79, respectively, which leads directly to the conclusion that the high He flow/pressure clusters present Au rich core/Cu rich shell structure but the low pressure clusters present Cu rich core/Au rich shell structure. The latter is expected to be more stable thermodynamically but crucially each can be produced in abundance.

In order to put the structure assignments on a more quantitative basis, we simulate the STEM intensity profiles of model core/shell morphologies. Simple geometrical structures were employed: both the core and the shell were spherical and the center of mass of the core coincided with the center of mass of the shell. The HAADF intensities were taken to depend exclusively on the height of the projected atomic column,[4,5,32] with each atom contributing a $Z^{1.32}$-dependent intensity.[33] We employed cluster diameters 3.78 and 3.32 nm, respectively, for the high He flow/pressure and low He flow/pressure samples and whole cluster composition of 5% and 43% as above. We assumed the diameters of the core remained the same as pure Au (1.58 nm) and pure Cu (2.61 nm) cores respectively for the high He flow/pressure and low He flow/pressure samples. The Au (for high He flow/pressure sample) or Cu (for He flow/pressure sample) ratio of the core was varied from 100% to 0% in 20% decrement. The remaining Au (or Cu) atoms were distributed uniformly in the shell when the composition of the core varied. The simulation results are displayed in Figure 2c,d. For high He flow/pressure sample, Figure 2c, the HAADF intensity of simulated profiles increased around the central area and formed a step when the Au ratio of core was higher than 20% ($Cu_{0.8}Au_{0.2}/Cu_{0.96}Au_{0.04}$). Comparing the quantitative values, we can see that the HAADF intensity of the experimental profile increases abruptly by 2.3 times in the central area. This value is higher than that of the simulated profile of $Cu_{0.2}Au_{0.8}/Cu_{0.99}Au_{0.01}$ cluster (2.1 times) and similar to the simulated profile of pure Au/pure Cu cluster (2.4 times). It means the high He flow/pressure sample is at least composed of Au rich/Cu rich clusters. As shown in Figure 2d, for the low He flow/pressure sample, the HAADF intensity of simulated profiles in central section increases and forms a crown structure when the Cu ratio reduces to 80% ($Cu_{0.8}Au_{0.2}/Au_{0.68}Cu_{0.32}$). The pattern is significantly different to the experimental profile of low He flow/pressure sample. Instead, the experimental profile is similar to the simulated profile of the pure Cu/pure Au cluster. The close resemblance between the simulated profiles of pure Au/pure Cu clusters and experimental data confirms that the high He flow/pressure sample has Au rich/Cu rich core/shell structure and the low He flow/pressure sample has Cu rich/Au rich core/shell structure.

Our results show that flow rate of the condensation gas plays a very important role during the formation of the clusters, leading to the observed tunability of the core/shell structures. The effect can be explained qualitatively by the following picture. The growth of clusters occurs in two stages in the gas-condensation technique: the energetic sputtered atoms from the sputtered target atoms are cooled by the He gas leading to the formation of seed clusters, then the nucleation of these seeds is followed by growth into larger, nanoscale clusters if and when the seeds reach a critical size.[31,37] Three-body collisions between two metal atoms and a cooling He atom are essential to remove excess kinetic energy from the sputtered atoms for the formation of seeds. In addition, the kinetic energy of the sputtered Cu atoms is

higher than that of the Au atoms due to the higher energy transfer function[38,39] and lower bond energy.[40] So under conditions of high He flow/pressure, both Au and Cu seeds are formed in abundance but, unlike the Au seeds, the Cu seeds are not stable enough to reach the critical size and thus growing into stable nm-size Cu particles. The Cu atoms instead attach to Au nuclei to form Au rich/Cu rich core/shell clusters (presumably metastable). When the He flow/pressure is reduced, the rate of nucleation is reduced but a small of stable nm-size Cu clusters form. Attachment of Au atoms generates Cu rich/Au rich core/shell clusters observed. This picture is supported by the fact that we do not observe any pure Cu clusters at high He flow/pressure, whereas a small number of large Cu clusters are observed at low pressure Figure 1b. The lack of Au rich/Cu rich core/shell clusters in low He flow/pressure sample may be because they lie outside the selected mass range. Of course, theoretical calculation to test this qualitative scheme, which does account for the results observed, would be most valuable.

In summary, we have demonstrated that by controlling the condensation conditions, we can prepare and deposit both Cu rich/Au rich, Au rich/Cu rich mass-selected, stable core/shell clusters of well-defined size with the RF magnetron-sputtering gas phase synthesis method. The work provides a method to create model bimetallic nanoparticles for catalysis, optics and magnetics and also provides understanding of the growth kinetics of these bimetallic clusters.

■ AUTHOR INFORMATION

Corresponding Author
R.E.Palmer@bham.ac.uk

■ ACKNOWLEDGMENT

■ REFERENCES

(1) Russell, A. E.; Rose, A. *Chem. Rev.* **2004**, *104*, 4613.
(2) Burda, C.; Chen, X. -B.; Narayanan, R.; El-Sayed, M. A. *Chem. Rev.* **2005**, *105*, 1025.
(3) Wilcoxon, J. P.; Abrams, B. L. *Chem. Soc. Rev.* **2006**, *35*, 1162.
(4) Ferrando, R.; Jellinek, J.; Johnston, R. L. *Chem. Rev.* **2008**, *108*, 845.
(5) Li, Z. Y.; Wilcoxon, J. P.; Yin, F.; Chen, Y.; Palmer, R. E.; Johnston, R. L. *Faraday Discuss.* **2008**, *138*, 363.
(6) Habas, S. E.; Lee, H.; Radmilovic, V.; Somorjai, G. A.; Yang, P. *Nat. Mater.* **2007**, *6*, 692.
(7) Tao, F; Grass, M. E.; Zhang, Y.; Butcher, D. R.; Renzas, J. R.; Liu, Z.; Chung, J. Y.; Mun, B. S.; Salmeron, M.; Somorjai, G. A. *Science* **2008**, *322*, 932.
(8) Piccinin, S.; Zafeiratos, S.; Stampfl, C.; Hansen, T. W.; Hävecker, M.; Teschner, D.; Bukhtiyarov, V. I.; Girgsdies, F.; Knop-Gericke, A.; Schlögl, R.; Scheffler, M. *Phys. Rev. Lett.* **2010**, *104*, 035503.
(9) Alayoglu, S.; Eichhorn, B. *J. Am. Chem. Soc.* **2008**, *130*, 17479.
(10) Peng, Z. M.; Yang, H. *J. Am. Chem. Soc.* **2009**, *131*, 7542.
(11) Liz-Marzán, L. M. *Langmuir* **2006**, *22*, 32.
(12) Kim, S.; Kim, S. K.; Park, S. *J. Am. Chem. Soc.* **2009**, *131*, 8380.
(13) Zitoun, D.; Respaud, M.; Fromen, M. C.; Casanove, M. J.; Lecante, P.; Amiens, C.; Chaudret, B. *Phys. Rev. Lett.* **2002**, *89*, 037203.

(14) Vasquez, Y.; Sra, A. K.; Schaak, R. E. *J. Am. Chem. Soc.* **2005**, *127*, 12504.
(15) Alloyeau, D.; Ricolleau, C.; Mottet, C.; Oikawa, T.; Langlois, C.; Le Bouar, Y.; Braidy, N.; Loiseau, A. *Nat. Mater.* **2009**, *8*, 940.
(16) Rao, C. N. R.; Kulkarni, G. U.; Thomas, P. J.; Edwards, P. P. *Chem. Soc. Rev.* **2000**, *29*, 27.
(17) Binder, W. H. *Angew. Chem., Int. Ed.* **2005**, *44*, 5172.
(18) Li, X.; Kiran, B.; Li, J.; Zhai, H.; Wang, L. -S. *Angew. Chem., Int. Ed.* **2002**, *41*, 4786.
(19) Konno, T. J.; Yamamuro, S.; Sumiyama, K. *J. Vac. Sci. Technol. B* **2002**, *20*, 834.
(20) Palmer, R. E.; Pratontep, S.; Boyen, H. G. *Nat. Mater.* **2003**, *2*, 443.
(21) Neukermans, S.; Janssens, E.; Chen, Z. F.; Silverans, R. E.; Schleyer, P. v. R.; Lievens, P. *Phys. Rev. Lett.* **2004**, *92*, 163401.
(22) Yin, F.; Xirouchaki, C.; Guo, Q.; Palmer, R. E. *Adv. Mater.* **2005**, *17*, 731.
(23) Wang, L. M.; Bulusu, S.; Zhai, H.; Zeng, X.; Wang, L. -S. *Angew. Chem., Int. Ed.* **2007**, *46*, 2915.
(24) Vajda, S.; Lee, S.; Sell, K.; Barke, I.; Kleibert, A.; von Oeynhausen, V.; Meiwes-Broer, K. H.; Rodríguez, A. F.; Elam, J. W.; Pellin, M. M.; Lee, B.; Seifert, S.; Winans, R. E. *J. Chem. Phys.* **2009**, *131*, 121104.
(25) Kaden, W. E.; Wu, T.; Kunkel, W. A.; Anderson, S. L. *Science* **2009**, *326*, 826.
(26) Lei, Y.; Mehmood, F.; Lee, S.; Greeley, J. P.; Lee, B.; Seifert, S.; Winans, R. E.; Elam, J. W.; Meyer, R. J.; Redfern, P. C.; Teschner, D.; Schlögl, R.; Pellin, M. J.; Curtiss, L. A.; Vajda, S. *Science* **2010**, *328*, 224.
(27) Cui, L. -F.; Huang, X.; Wang, L. -M.; Li, J.; Wang, L. —S. *Angew. Chem., Int. Ed.* **2007**, *46*, 742.
(28) Yin, F.; Lee, S.; Abdela, A; Vajda, S.; Palmer, R. E. *J. Chem. Phys.* **2011**, *134*, 141101.
(29) Carroll, S. J.; Nellist, P. D.; Palmer, R. E.; Hobday, S.; Smith, R. *Phys. Rev. Lett.* **2000**, *84*, 2654.
(30) Carroll, S. J.; Pratontep, S.; Streun, M.; Palmer, R. E.; Hobday, S.; Smith, R. *J. Chem. Phys.* **2000**, *113*, 7723.
(31) Pratontep, S.; Carroll, S. J.; Xirouchaki, C.; Streun, M.; Palmer, R. E. *Rev. Sci. Instrum.* **2005**, *76*, 045103.
(32) Li, Z. Y.; Young, N. P.; Di Vece, M.; Palomba, S; Palmer, R. E.; Bleloch, A. L.; Curley, B. C.; Johnston, R. L.; Jiang, J.; Yuan, J. *Nature* **2008**, *451*, 46.
(33) Wang, Z. W.; Toikkanen, O.; Yin, F.; Li, Z. Y.; Quinn, B. M.; Palmer, R. E. *J. Am. Chem. Soc.* **2010**, *132*, 2854.
(34) Voyles, P. M.; Muller, D. A.; Grazul, J. L.; Citrin, P. H.; Gossmann, H.-J. L. *Nature* **2002**, *416*, 826.
(35) van Schooneveld, M. M.; Gloter, A.; Stephan, O.; Zagonel, L F.; Koole, R.; Meijerink, A.; Mulder, W. J. M.; de Groot, F. M. F. *Nat. Nanotechnol.* **2010**, *5*, 538.
(36) Greenwood, N. N.; Earnshaw, A. *Chemistry of the Elements*, 2nd ed.; Butterworth-Heinemann: Oxford, 1997.
(37) Granqvist, C. G.; Buhrman, R. A. *J. Appl. Phys.* **1976**, *47*, 2200.
(38) Chapman, B. *Glow Discharge Processes*; Wiley: New York, 1980.
(39) Konno, T. J.; Yamamuro, S.; Sumiyama, K. *J. Vac. Sci. Technol. B* **2002**, *20*, 834.
(40) *CRC Handbook of Chemistry and Physics*, 91st ed (Internet Version 2011); Haynes, W. M., Ed.; CRC Press/Taylor and Francis: Boca Raton, FL, 2011.